

# Measles Rash Image Detection Using Deep Convolutional Neural Network

Kimberly Glock<sup>1+</sup>, Charlie Napier<sup>1+</sup>, Andre Louie<sup>1</sup>, Todd Gary<sup>1</sup>, Joseph Gigante<sup>2</sup>, William Schaffner<sup>3</sup>, Qingguo Wang<sup>1\*</sup>

<sup>1</sup>College of Computing and Technology Lipscomb University, Nashville, TN, US

<sup>2</sup>Department of Pediatrics, Vanderbilt University School of Medicine, TN, US

<sup>3</sup>Department of Health Policy, Vanderbilt University School of Medicine, TN, US

<sup>+</sup>These authors contributed equally to this work

<sup>\*</sup>Corresponding Email: qwang@lipscomb.edu

**Abstract – Measles is extremely contagious and is one of the leading causes of vaccine-preventable illness and death in developing countries, claiming more than 100,000 lives each year. Measles was declared eliminated in the US in 2000. As a result, an increasing number of US healthcare professionals and the public have never seen the disease. Unfortunately, the Measles resurged in the US in 2019 with 1,282 confirmed cases. To assist in diagnosing measles, we created a dataset of more than 1300 images of a variety of skin conditions and utilized deep convolutional neural network to distinguish measles rash from other skin conditions. On our curated image dataset, our model reaches a classification accuracy 95.2%, a sensitivity 81.7%, and specificity 97.1%. Our model can potentially be used to facilitate an accurate and early detection of measles to help contain measles outbreaks.**

**Keywords — Measles, Measles Rash, Image Recognition, Deep Learning, Transfer Learning, Convolutional Neural Network, CNN, Residual Network.**

## I. INTRODUCTION

The measles virus is among the oldest recorded viruses that infect humans. According to the Centers for Disease Control and Prevention (CDC), the first scientific description occurred in the 9<sup>th</sup> century by Persian physician Rhazes, who identified it as a separate virus from smallpox and chickenpox [1]. In 1912, measles became a nationally notifiable disease in the United States, requiring healthcare providers and laboratories to report all diagnosed cases. In the first decade of reporting, an average of 6,000 measles-related deaths were reported each year. Before the measles vaccine was first introduced in 1963, it is estimated that 3 to 4 million people in the US were infected each year, with an estimated 400 to 500 of these cases resulting in death. Globally, before widespread vaccination, the virus caused 2 million to 3 million deaths per year [1].

Measles is an extremely contagious virus, it is estimated that up to 90% of people who are close to an infected individual will also contract the virus (assuming they aren't immune). Furthermore, infected individuals are capable of spreading the disease well before the skin rash even appears (as many as four days prior), thus increasing the risk of transmission even further [2].

Thanks to the implementation of the vaccine, measles was later declared eliminated from the US in 2000, where individual cases of measles would remain exceptionally rare for the next 19 years [1]. Despite the effectiveness of the vaccine, the virus resurged in the US in 2019 with a total 1,282 individual cases in 31 different states [3]. At the same time measles cases increased globally with more than 500,000 confirmed cases of measles and an estimated of 140,000 cases resulted in death [3].

With the virus continuing to spread worldwide, proper and efficient diagnosis of measles will be essential in mitigating the rate of infection. However, measles cases have been exceptionally rare in the US since its official elimination in 2000, and as a result diagnosing it has become more difficult, particularly for younger healthcare professionals who have never seen the disease before.

The most defining symptom of measles is the skin rash that it causes, as the other symptoms closely mimic other illnesses. The distinctive pattern of the rash, as well as the method in which the rash progresses across the body are critical signs that healthcare providers make use of to visually diagnose the disease. Without immediate medical attention, complications can occur such as inflammation of the brain, loss of hearing, and pneumonia.

The goal of this study is to leverage deep convolutional neural networks (CNNs) to assist physicians and patients alike in the identification and possible diagnosis of the disease. Currently, there are no other existing algorithms designed specifically for the visual detection of the measles rash. A model capable of measles rash characterization can be applied to many fields. It could be deployed as an application to be used in telemedicine, airport security to prevent transmission of the disease, or potentially as a phone application in developing countries, where health workers are scarce, to facilitate the recognition of measles.

## II. RELATED WORK

The deep convolutional neural networks (CNNs) were inspired by the structure and organization of the visual cortex in cats and monkeys. CNNs are composed of stacks

**Table 1:** Example deep CNN models emerged recently for skin lesion classification<sup>+</sup>

No.	Skin condition	Deep CNN models	Dataset	Ref.
1	Cancer-related skin lesion	DenseNet-169	HAM10000	[16]
2	Twenty-six most common skin conditions	Inception-v4, an Inception-ResNet	De-identified cases from a teledermatology practice serving 17 clinical sites	[17]
3	Erythema migrans rashes in early Lyme disease	ResNet50	A dataset of 1834 images, including 1718 expert clinician-curated online images	[18]
4	Eleven skin conditions including measles rash	ResNet34	A dataset of 587 images	[19]*
5	Skin cancer	Alex-net	MED-NODE, Derm (IS & Quest) and ISIC	[20]
6	Melanoma and other skin lesions	PNASNet-5, InceptionV4, InceptionResNetV2, SENet154	ISIC 2018 challenge dataset	[21]
7	Melanoma and other skin lesions	EfficientNets and other models	HAM10000, BCN_20000, and MSK dataset	[22]

<sup>+</sup>Only the work published in 2019 (or early 2020) were included and this list was not intended to be exhaustive.

\* This study was described in an online poster [19].

of processing layers, which enable them to learn complex features from imaging data. Due to the outstanding performances in solving many computer vision problems, CNNs have gained tremendous attention in recent years and have been applied increasingly widely in medical research and radiology [5][8][9]. For example, Nasr-Esfahani *et al.* developed a CNN model for detecting melanoma, with a predictive accuracy of 81% [5]. More recently, to address the most common skin conditions seen in primary care, Google developed a CNN-based system with an accuracy on par with U.S. board-certified dermatologists [17]. CNNs have also been employed to study other diseases, such as breast cancer, diabetic retinopathy, and lymph node metastasis [8][9][16][18].

CNN requires sufficient data and computational resources for model training. If only a small image dataset is available, special strategies, e.g. data augmentation or transfer learning, are often used to increase the performance of classification. Transfer learning utilizes a pretrained model to solve a different but related problem [12] [13]. Compared to approach of building a deep CNN from scratch, it requires fewer training images and reduced runtime as a result. A recent comparative study showed on a small dataset, transfer learning is more useful than other methods investigated [8]. In another study that utilized transfer learning to develop a CNN model, Kermany *et al.* demonstrated performance comparable to that of human experts in classifying age-related macular degeneration and diabetic macular edema [9].

Stimulated by crucial need for early diagnosis and treatment of diseases and a shortage of dermatologists, many CNN-based systems were developed for classifying skin photographs [16-22]. Table 1 shows 7 CNN-based methods emerged lately for skin lesion classification. They all utilized transfer learning to obtain final models. For instance, the studies in rows 3 and 4 employed residual networks (ResNet) to construct CNNs. The 4<sup>th</sup> study in Table 1, which was presented in a poster, used ResNet34

to distinguish 11 skin conditions and rashes. Although measles rash was among the 11 skin conditions, the evidence (and accuracy) of measles identification was not reported by developers. Apart from this work, we are not aware of other recent study of measles rash detection.

With the lack of tools for visual recognition of measles and the resurgence of measles in the US in 2019, the cause of which was linked to travel-related transmissions with subsequent spread through undervaccinated populations [7], the models that can accurately detect measles rash are urgently needed. Improved capability of measles rash identification would help healthcare professionals to effectively address new and varied challenges in the US posed by the potential reemergence of measles into populations.

The rest of the paper is organized as follows. First, we describe our data and CNN model. Next, we provide our experimental results. Lastly, Section V offers discussion and directions for future development.

### III. MATERIALS AND METHODS

#### *Data collection*

To analyze photographic rash images and accurately identify the measles rash from normal skin and other dermatological issues, we built our CNN models in a binary classification context, such that all the images are labeled as either “Measles” or “Non-Measles.” For the non-measles subgroup in particular, it is important to have a dataset including classes similar to the measles rash in appearance as well as classes that significantly differ, in order to provide overall diversity to the dataset.

As there are no public resources available that contain an extensive library of measles images specifically, we collected the data for our study using the Bing Web Search API (part of the Microsoft Azure package) to parse images from the web. The dataset contains rash images of 11 different disease states: Bowens disease, chickenpox,

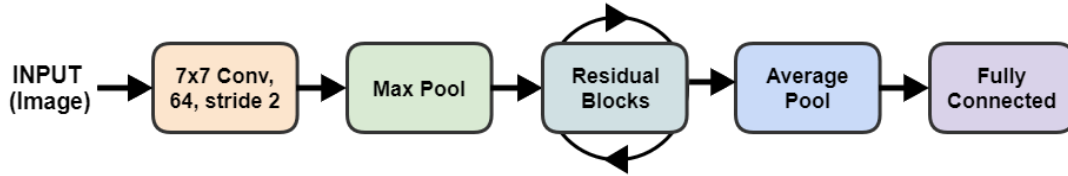


Figure 1: Basic processes of ResNet

chigger bites, dermatofibroma, eczema, enterovirus, keratosis, measles, psoriasis, ringworm and scabies. Additionally, images of normal skin are also included in the dataset. Table 2 shows the complete list of samples we collected. In total, there are 158 images of the measles rash, and 1158 non-measles images present in the dataset.

Table 2: Data set description

Image Classes	Number of Images
Bowen's Disease	124
Chickenpox	170
Chigger Bites	87
Dermatofibroma	80
Eczema	95
Enterovirus	117
Keratosis	112
Measles	158
Normal Skin	41
Psoriasis	122
Ringworm	131
Scabies	79
<b>Total</b>	<b>1316</b>

Two clinicians at Vanderbilt University, Dr. Joseph Gigante and Dr. William Schaffner, who are also co-authors of this paper, assisted us with data collection and curation. Dr. Schaffner, an infectious disease specialist, consulted with us in the preliminary stages of the study and provided several medical links to use for parsing measles images. Dr. Gigante, a pediatrician, reviewed the measles images prior to training the model and advised which were more than likely the measles. Ultimately, only the images he approved of were used.

Building a deep CNN model from scratch typically requires a very large dataset, i.e. at least 1000 images per class, in order to produce accurate classification results. To mitigate the limited availability of usable measles images for training and testing, we experimented with image augmentation strategies in the early phase of our study, to create duplicates of measles images with minor adjustments such as random rotations and horizontal flips. Our benchmark analysis showed, however, our final model, which was adapted from a pretrained model, provided better performance without the use of augmentation.

### Method

On our dataset, we experimented with three well-known CNN architectures in the field: VGG-16 [15] and two deep residual networks (ResNet), ResNet34 and ResNet50 [11]. VGG-16 consists of convolutional layers, max pooling layers, activation layers, and fully connected layers, but only 16 of them have weights (and, hence, its name came from) [15]. ResNet was the winner of the 2015 ImageNet Large Scale Visual Recognition Challenge (ILSVRC 2015) in image classification, detection, and localization. In the COCO 2015 competitions, ResNet also won the 1st place on the tasks of ImageNet detection, localization, etc. ResNet50 stands for 50-layer residual networks. Both ResNet34 and ResNet50 were already pretrained on ImageNet, a very large dataset that contains over 14 million images [23].

Figure 1 illustrates the basic processes that take place in a ResNet. There are 5 stages in a ResNet, each with a convolution block. Stage 1 consists of convolution and max pooling layers. A convolutional layer uses a filter called a kernel to pass over image to create a feature map. The initial kernel size is 7x7 with 64 output channels and a stride of 2. Max pooling reduces image size by keeping the max value of each matrix square that the kernel passes over. Stages 2-5 are residual blocks. Residual blocks are special highway networks without gates in their skip connections to allow information flow from the initial layers to the final layers. Following stage 5, there is an average pooling and a fully connected layer. Average pooling reduces image size by using the average value of each matrix square. The fully connected layer takes the end result of the convolution and pooling and outputs the final probabilities for image classification.

As stated earlier, because the two image classes in our dataset are imbalanced, we also tried oversampling and image augmentation techniques using the keras library [14]. Our benchmark analysis indicated that the ResNet50 model without augmentation provided the best results. Thus, we will just discuss ResNet50 hereafter. A diagram of ResNet50 is provided in Appendix A. With ResNet50 being already tuned for recognizing features of various images, we only need to adapt the last part of ResNet50 to enable it to classify measles rashes.

ResNet50 and several other deep ResNet models were first published in 2015 by Microsoft Asia, and have since seen many successful applications [9][17-19]. The version of ResNet50 utilized in this study is the latest

implementation (2020) in a Python package fastai [10]. In fastai, ResNet50 is layered on top of the Pytorch library, a Python environment in fastai. For a full documentation of the fastai library, interested readers are referred to [10].

#### IV. RESULTS

##### Model training and testing

A stratified 5-fold cross validation was conducted to train the model. Firstly, we kept all the convolutional layers, i.e. the backbone of the model, with their weights pretrained on ImageNet and trained only the last few layers of the model. For each round of training, the images were divided randomly into training and validation sets with an 80/20% split, respectively. Batch normalization was applied to model training. We set batch size to be 64 and the number of epochs to be 8 for the initial phase of model training.

Each image in our dataset was classified into one of the two classes: measles (positive) and non-measles (negative). On each iteration, we calculated three commonly used metrics to evaluate our method: sensitivity, specificity and accuracy, which are defined as follows:

$$\begin{aligned} \text{sensitivity} &= TP / (TP + FN) , \\ \text{specificity} &= TN / (TN + FP) , \\ \text{accuracy} &= (TP + TN) / (TP + FN + TN + FP), \end{aligned}$$

where TP, TN, FP and FN denote the number of true positive, true negative, false positive and false negative classifications, respectively.

After the 5 iterations, the average performances of the models on validation sets were computed. Table 3 below provides the three computed metrics. It shows the average accuracy, sensitivity, and specificity of our model are 94.8%, 74.1%, and 97.6%, respectively.

**Table 3:** Results of 5-Fold cross validation

Iteration	Sensitivity (%)	Specificity (%)	Accuracy (%)
1	83.87	96.54	95.04
2	78.13	96.98	94.70
3	67.74	98.70	95.04
4	68.75	97.84	94.32
5	71.88	97.84	94.70
<b>Average</b>	<b>74.07</b>	<b>97.58</b>	<b>94.76</b>

##### Model refinement

After creating the initial model, we then fine-tuned the whole model by unfreezing backbone layers of the model for retraining. As learning rate affects model performance greatly, to find consensus learning rates for the five cross-validation iterations, we visualized the relationship between learning rate and loss function on each iteration. Figure 2 provides one example plot we created on an iteration.

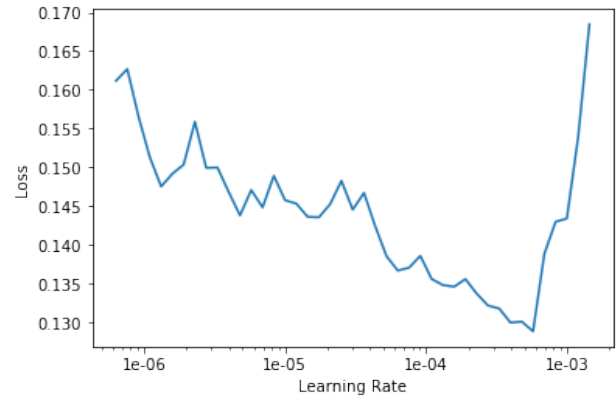


**Figure 2:** Values of the loss function vs learning rate

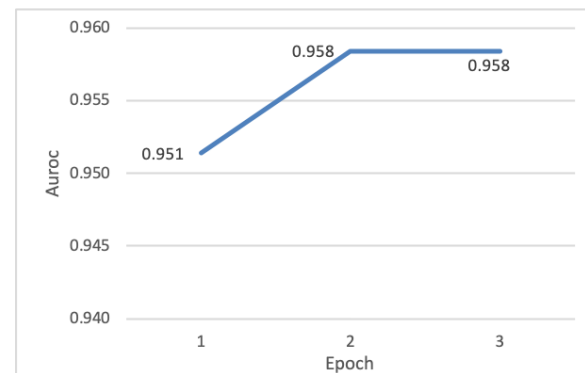
It shows in Figure 2 that the recorded loss tended to decrease with the increase of learning rate, before it diverges quickly after a point close to 1e-3. Based on this observation as well as four other similar plots, we specified the range [1e-6, 1e-4] as our differential learning rates for model refinement, with which three epochs were then performed to obtain our final model.

Table 4 provides the performance of our final model on the validation sets. It shows model refinement improved the sensitivity significantly, from original 74.1% to 81.7%.

**Table 4:** Results of our final model

Iteration	Sensitivity (%)	Specificity (%)	Accuracy (%)
1	87.10	96.10	95.04
2	84.38	96.55	95.08
3	80.65	98.27	96.18
4	71.88	96.12	93.18
5	84.38	98.28	96.59
<b>Average</b>	<b>81.67</b>	<b>97.06</b>	<b>95.21</b>

We also computed the average area under the curve (AUC) score based on the receiver operator characteristic (ROC) curve. Figure 3 below shows the improvement of the AUC score in the process of model refinement.



**Figure 3:** Improvement of the area under the curve (AUC) score in the process of model refinement

To verify our results, we manually examined some misclassified images. Figure 4 provides an example of a false positive prediction. The left photo in Figure 4 is enterovirus rash, in comparison with a measles rash on the right in Figure 4. This example shows the challenge of distinguishing the measles rash from other skin conditions. As the majority of false positive classifications were made on images very similar in appearance to the measles rash, such as the enterovirus rash in Figure 4, to further minimize such error, more training images of both the measles rash and these similar subclasses are required.

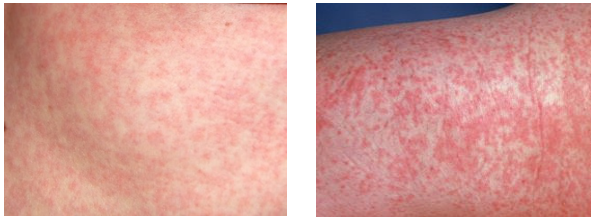


**Figure 4:** Examples of a false positive prediction (left) and a false negative prediction (right)

## V. CONCLUSIONS AND FUTURE WORK

With the spread of the measles virus continuing to increase worldwide, and fewer healthcare providers in the US that can accurately identify it due to its rarity in recent decades, a properly trained model capable of identifying measles rash is essential in combatting the outbreak.

In this paper, we used deep convolutional neural network (CNN) to distinguish the distinctive measles rash from a variety of other skin conditions. The proposed method showed promising results with an average accuracy of 95.2% and an average sensitivity of 81.7%. Given the small size of the dataset used, the performance can be improved with the addition of more images. The model can be further enhanced by expending the dataset to include a larger spectrum of rash illnesses in children, e.g. rubella, drug-induced rash, roseola, erythema infectiosum, toxic shock syndrome, Kawasaki disease as well as the newly-recognized multisystem inflammatory syndrome in children, along with others.

Our CNN model focuses on the appearance of the rash and does not take into account the distribution of the rash on the body and its development (the measles rash characteristically begins on the head/face and then spreads down the body). Moreover, we did not include information about other concurrent symptoms, e.g. whether the patient has a fever or the classic “3Cs” of measles: cough, coryza and conjunctivitis, due to the unavailability of the data. Such information, when available in the future, can be easily integrated into our model to improve diagnosis efficacy further.

Our dataset possesses a variety of age, gender, and body parts across samples, but does not have a wide

diversity of skin color. Currently, the dataset is predominately composed of images of Caucasian skin, with fewer than 20 images representing minority skin tones. So a future development of this study is to obtain more ethnically diverse images to use for model re-training. By incorporating more images from diverse ethnical groups, our model can be further improved and more importantly it can be more readily deployed in telemedicine to aid healthcare providers in diagnosis.

Another future development is to create a phone application that can identify the measles rash. With a growing generation of younger doctors that utilize smart technology in the field, a phone-based application could serve as a powerful tool in the diagnosis of the disease.

## REFERENCES

- [1] Centers for Disease Control and Prevention. (2018). *Measles (Rubeola) Pre-vaccine Era*. Retrieved from <https://www.cdc.gov/measles/about/history.html>
- [2] Centers for Disease Control and Prevention. (2018). *Measles (Rubeola) Transmission of Measles*. Retrieved from <https://www.cdc.gov/measles/transmission.html>
- [3] Centers for Disease Control and Prevention. (2020). *Measles (Rubeola) Measles Cases and Outbreaks*. Retrieved from <https://www.cdc.gov/measles/cases-outbreaks.html>
- [4] Suzuki, K. (2017). Overview of deep learning in medical imaging. *Radiological physics and technology*, 10(3), 257-273.
- [5] Nasr-Esfahani, E., Samavi, S., Karimi, N., Soroushmehr, S. M. R., Jafari, M. H., Ward, K., & Najarian, K. (2016, August). Melanoma detection by analysis of clinical images using convolutional neural network. In *2016 38th Annual International Conference of the IEEE Engineering in Medicine and Biology Society (EMBC)* (pp. 1373-1376). IEEE.
- [6] Kawahara, J., BenTaieb, A., & Hamarneh, G. (2016, April). Deep features to classify skin lesions. In *2016 IEEE 13th International Symposium on Biomedical Imaging (ISBI)* (pp. 1397-1400). IEEE.
- [7] Pauls, C. I., Marston, H. D., & Fauci, A. S. (2019). Measles in 2019 - Going Backward. *New England Journal of Medicine*, 380(28), 2185-2187.
- [8] Yadav, S.S., Jadhav, S.M. Deep convolutional neural network based medical image classification for disease diagnosis. *J Big Data* 6, 113 (2019). <https://doi.org/10.1186/s40537-019-0276-2>
- [9] Kermany DS, Goldbaum M, Cai W, Valentim CC, Liang H, Baxter SL, McKeown A, Yang G, Wu X, Yan F, et al. Identifying medical diagnoses and treatable diseases by image-based deep learning. *Cell*. 2018;172(5):1122–31.
- [10] fastai. (2020). *fastai*. Retrieved from <https://docs.fast.ai/>
- [11] He, K., Zhang, X., Ren, S., & Sun, J. (2016). Deep residual learning for image recognition. In *Proceedings of the IEEE conference on computer vision and pattern recognition* (pp. 770-778).
- [12] West, Jeremy; Ventura, Dan; Warnick, Sean (2007). Spring Research Presentation: A Theoretical Foundation for Inductive Transfer. Brigham Young University, College of Physical and Mathematical Sciences.
- [13] George Karimpanal, Thommen; Bouffanais, Roland (2019). Self-organizing maps for storage and transfer of knowledge in reinforcement learning. *Adaptive Behavior*. 27 (2): 111–126. 08318.
- [14] Chollet, F., et al., Keras, <https://keras.io>, 2015.
- [15] K. Simonyan and A. Zisserman. (2015) Very deep convolutional networks for large-scale image recognition. International Conference on Learning Representations (ICLR). arXiv preprint *arXiv:1409.1556*
- [16] Mobiny A, Singh A, Van Nguyen H. (2019) Risk-Aware Machine Learning Classifier for Skin Lesion Diagnosis. *J Clin Med*. 8(8) 1241, doi: 10.3390/jcm8081241.

[17] Liu, Y., *et al.* (2019) a deep learning system for differential diagnosis of skin diseases. arXiv:1909.05382.

[18] Burlina PM, Joshi NJ, Ng E, Billings SD, Rebman AW, Aucott JN. (2019) Automated detection of erythema migrans and other confounding skin lesions via deep learning. *Comput Biol Med.*, 105:151-156.

[19] S. Sharma (2019) DermaDetect: A computer vision and deep learning approach for an accurate diagnosis of skin conditions and rashes. DOI: 10.13140/RG.2.2.11636.91522. Retrieved from <https://www.researchgate.net/publication/335083461>

[20] Hosny KM, Kassem MA, Foaud MM (2019) Classification of skin lesions using transfer learning and augmentation with Alex-net. *PLoS ONE* 14(5): e0217293.

[21] Md Ashrafal Alam Milton (2019) Automated Skin Lesion Classification Using Ensemble of Deep Neural Networks in ISIC 2018: Skin Lesion Analysis Towards Melanoma Detection Challenge. arXiv:1901.10802.

[22] N. Gessert, M. Nielsen, M. Shaikh, R. Werner, A. Schlaefler (2020) Skin lesion classification using ensembles of multi-resolution EfficientNets with meta data. *MethodsX*. vol 7, 100864

[23] L. Fei-Fei (2010) ImageNet: crowdsourcing, benchmarking & other cool things, CMU VASC Seminar.

## APPENDICES

### Appendix A: Complete Resnet50 Architecture

